Analytical and Bioanalytical Chemistry
https://doi.org/10.1007/s00216-024-05356-z

RESEARCH PAPER

Electrogenerated chemiluminescence from luminol-labelled microbeads triggered by in situ generation of hydrogen peroxide

Andrea Fiorani[1] · Claudio Ignazio Santo[2] · Kohei Sakanoue[1] · Donato Calabria[2] · Mara Mirasoli[2] · Francesco Paolucci[2] · Giovanni Valenti[2] · Yasuaki Einaga[1]

Received: 4 April 2024 / Revised: 11 May 2024 / Accepted: 21 May 2024

Abstract

We developed a sensing strategy that mimics the bead-based electrogenerated chemiluminescence immunoassay. However, instead of the most common metal complexes, such as Ru or Ir, the luminophore is luminol. The electrogenerated chemiluminescence of luminol was promoted by in situ electrochemical generation of hydrogen peroxide at a boron-doped diamond electrode. The electrochemical production of hydrogen peroxide was achieved in a carbonate solution by an oxidation reaction, while at the same time, microbeads labelled with luminol were deposited on the electrode surface. For the first time, we proved that was possible to obtain light emission from luminol without its direct oxidation at the electrode. This new emission mechanism is obtained at higher potentials than the usual luminol electrogenerated chemiluminescence at 0.3–0.5 V, in conjunction with hydrogen peroxide production on boron-doped diamond at around 2–2.5 V (*vs* Ag/AgCl).

Keywords Electrogenerated chemiluminescence · Luminol · Hydrogen peroxide · Carbonate · Microbeads · Boron-doped diamond

Introduction

The development of sensing strategies for analytical purpose relies significantly on the transduction method for the outcome detection and the overall sensitivity of the technique [1, 2]. Electrogenerated chemiluminescence (ECL) is one of the electroanalytical methods that applied to biosensing had the most impact on the field.

Combining the concepts of electrochemistry with chemiluminescence, the electrogenerated chemiluminescence is a phenomenon in which light emission results from a chemical reaction that takes place at an electrode surface during an electrochemical process. Reactive intermediates are electrochemically generated, and the following transfer of electrons enables the formation of emitting excited states [3].

Compared to other luminescence-based methods, like fluorescence or chemiluminescence, ECL has several benefits, including a superior signal-to-noise ratio, a broad dynamic range, and compatibility with biological samples. This promoted the commercialization of analyzer based on ECL technology for drug discovery, environmental monitoring, and diagnostics [4–6].

Because ECL emission is primarily triggered by an electrochemical reaction [7], stable and electrochemically reversible inorganic complexes are favorably used, especially Ru and Ir derivatives [8–11], in combination with their notable quantum yield of emission [12, 13].

On the other hand, organic molecules are generally preferred in CL with oxalate esters and sterically stabilized 1,2-dioxetane that have been utilized [14], although the use of organic molecules in ECL had experienced a resurgence [15, 16].

Luminol, the 5-amino-2,3-dihydrophtalazine-1,4-dione, is an organic molecule that has received an extended

Published in the topical collection *Optical Biosensors and Biomimetic Sensors for Chemical Analysis* with guest editors Elena Benito-Peña and Guillermo Orellana.

In honor of Professor María Cruz Moreno Bondi.

✉ Andrea Fiorani
andrea.fiorani@keio.jp

✉ Yasuaki Einaga
einaga@chem.keio.ac.jp

[1] Department of Chemistry, Keio University, Yokohama 223-8522, Japan

[2] Department of Chemistry "G. Ciamician", University of Bologna, 40126 Bologna, Italy

Published online: 04 June 2024

investigation for application in both CL [17–19] and ECL [20–23]. Generally, luminol is free to diffuse in solution, and this defines the chemical reactions involved in the ECL emission [24]. In particular, luminol can be oxidized at the electrode to generate ECL, with enhanced emission in the presence of hydrogen peroxide [25, 26]. This enabled a wide range of (bio)analytical testing, for example, by enzymes, where substrate conversion releases hydrogen peroxide [27].

On the other hand, restricted diffusion is typical of various analytical methods where the luminophore is fixed to a biorecognition element, in case of ECL far from the electrode surface preventing direct electron transfer. Generally, this is obtained by coating the biorecognition element onto microbeads or well microtiter plates, which technological applications are found in Elecsys or Meso Scale Discovery analyzers, respectively [5, 6].

The ECL immunoassay stands as a key technology for the sensitive and precise detection of markers or biomarkers in diagnostic analysis. Generally, the luminophore is $[Ru(bpy)_3]^{2+}$, or Ir complexes with ligand derivatives, and the ECL emission is triggered exclusively by radicals generated through the oxidation of the coreactant in a sequence of electrochemical and chemical reaction known as *heterogeneous coreactant mechanism* [28–34].

In our case, luminol has been bound to paramagnetic microbeads mimicking the approach used in commercial instruments widely employed in clinical analysis (Fig. 1) [34]. These microbeads are attracted to the electrode surface by a magnet, and the following electrochemical generation of H_2O_2 directly in situ triggers the ECL emission. The H_2O_2 in situ generation proceeds through a sequence of electrochemical oxidation and chemical reactions of carbonate electrolyte at a boron-doped diamond (BDD) electrode [35, 36]. The emission from luminol has also been detected by ECL imaging which has proven to be effective in examining species on the electrode surface, enabling the resolution of spatially and temporally electrochemical signals from surrounding background signals [20, 29, 30, 37, 38].

Here, we demonstrated that when luminol is not free to diffuse in solution, the ECL emission in conjunction with its direct electrochemical oxidation at the electrode is not observed, and we infer that the ECL generation follows an alternative pathway involving an exclusive chemical oxidation by H_2O_2 generated from carbonate oxidation.

Materials and methods

Chemicals

ChromPure Mouse immunoglobulin (IgG: 5.7 mg ml^{-1}) was obtained from Jackson ImmunoResearch (West Grove, PA). Biotinamidohexanoic acid N-hydroxysuccinimide ester, sodium periodate, N-(4-Aminobutyl)-N-ethylisoluminol (ABEI), Tween 20, and sodium carbonate were obtained from Sigma-Aldrich (St. Louis, MO). Potassium dihydrogen phosphate (KH_2PO_4, ≥ 99.5%), dipotassium hydrogen phosphate (K_2HPO_4, ≥ 99.0%), phosphoric acid (H_3PO_4, ≥ 85.0%), sodium perchlorate monohydrate ($NaClO_4 \cdot H_2O$, ≥ 98.0%), and dimethyl-sulfoxide (DMSO, super dehydrated, ≥ 99.0%) were obtained from Wako (Osaka, Japan). Paramagnetic microbeads Dynabeads MyOne Streptavidin T1 (diameter 1 µm, 10 mg mL^{-1}) were obtained from Thermo Fisher Scientific (Waltham, MA). Filters for dialysis Spectra-Por Float-A-Lyzer G2 were obtained from REPLIGEN (Waltham, MA). Double-distilled water with a maximum conductivity of 18.2 MΩ·cm was provided by a Simply-Lab water system (DIRECT-Q UV3, Millipore, Burlington, MA). All reagents were used as received.

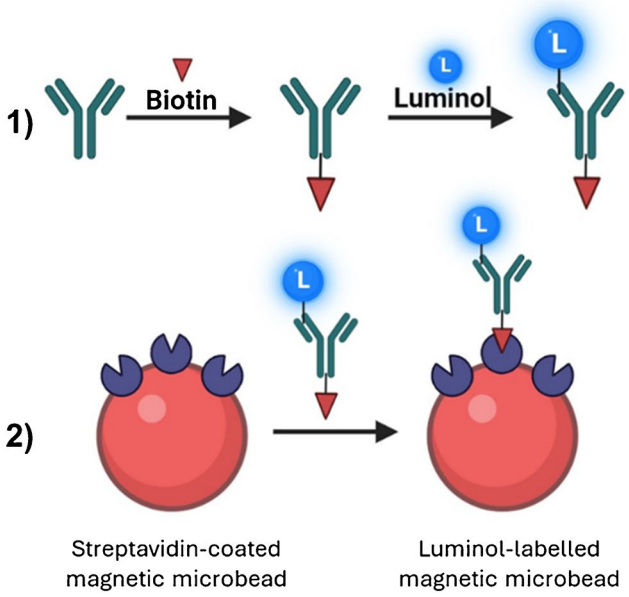

Fig. 1 Scheme of (1) antibody conjugation with biotin and luminol, and (2) labelling of the streptavidin-coated magnetic microbead with luminol conjugate

Preparation of the BDD electrodes

BDD films were deposited on silicon (111) wafers (Shinwa Tsusho, Japan) using a microwave plasma-assisted chemical vapor deposition (MPCVD) system (CORNES Technologies/ASTeX-5400), according to our previous procedure [34, 39]. Acetone and trimethyl borate were used as the carbon and boron sources, respectively, with a B/C atomic ratio of 1%. The surface morphology of BDD was examined with a field emission scanning electron microscope (SEM, JCM-6000, JEOL, Japan). Raman spectra of BDD were recorded

with an Acton SP2500 (Princeton Instruments) with an excitation wavelength of 532 nm (Figure S1).

Electrogenerated chemiluminescence imaging

ECL imaging measurements involved the use of a PTFE homemade electrochemical cell comprised of a 1% BDD working electrode (geometric area 3.5 cm^2), Pt wire counter electrode, and Ag/AgCl (3 M KCl) reference electrode. ECL image acquisition was performed with an ultrasensitive CCD camera (Atik Cameras 383L + Mono CCD Camera). The electrochemical cell and camera were enclosed in a dark box to avoid interferences from external light (Figure S2).

Electrogenerated chemiluminescence

Electrochemical measurements were conducted with a potentiostat PGSTAT302N (Metrohm). The poly(methyl methacrylate) cell is a single compartment (total volume 0.9 ml) with BDD as the working electrode (0.19 cm^2), a Pt disk counter electrode (0.072 cm^2), and a reference electrode Ag/AgCl (3 M NaCl). The ECL signals were measured with a photomultiplier tube (PMT, Hamamatsu R928) placed at a fixed height above the electrochemical cell. Both the electrochemical cell and the PMT were placed inside a dark box. A high-voltage power socket assembly with a transimpedance amplifier (Hamamatsu C6271) was used to supply the voltage to the PMT, using an external trigger connection to the potentiostat DAC module. Light/current/voltage curves were recorded by collecting the amplified PMT output signal with the ADC module of the potentiostat. For all experiments, the error bar shows the relative standard deviation (RSD) from 3 independent measurements.

Electrode pretreatment and cleaning

Prior to each measurement, the BDD surface was pretreated to guarantee reproducibility by anodic oxidation at + 3.5 V followed by cathodic reduction at − 3.5 V in 100 mM $NaClO_4$ solution, for a total fixed charge of 0.15 C cm^{-2} in each step.

Immunoglobulin conjugation with biotin and luminol

The following procedure was adapted from our previous publication [34]. Immunoglobulin G (IgG) was diluted to 2 mg ml^{-1} with 100 mM phosphate buffer (pH 8.5). Biotinamidohexanoic acid N-hydroxysuccinimide ester (0.03 mg) was dissolved in 50 µl DMSO and added to 1 ml of IgG and then stirred for 90 min at RT. IgG was diluted to 1 mg ml^{-1} with freshly prepared $NaIO_4$ (1 ml, 50 mM) in 100 mM phosphate buffer (pH 4.5, K^+ makes a precipitate) and incubated for 30 min in the dark [40]. Then, it was dialyzed at 4 °C overnight against 100 mM phosphate buffer (pH 7.5). The oxidized IgG was incubated with ABEI (100 µl, 50 mM) dissolved in 100 mM PB (pH 8.5) for 1 h. Then, it was dialyzed at 4 °C overnight against 100 mM phosphate buffer (pH 7.5).

Beads conjugation

Four microliters of beads from the original solution were washed three times with 100 mM phosphate buffer (pH 8). Then, they were incubated for 30 min with 200 µl of luminol-Ab conjugate. Washed three times with Tween 20 at 0.05% in 100 mM Na_2CO_3, and finally diluted to 20 µl with 100 mM Na_2CO_3 (5 µl for 1 measure).

Results and discussion

Our preliminary study involves the characterization of microbeads functionalized with luminol amino-derivate (Fig. 1). These functionalized beads offered a significant advantage by presenting a higher density of active sites, enabling high luminol loading. To comprehensively evaluate the electrogenerated chemiluminescence (ECL) emission properties, we employed ECL imaging with a charge-coupled device (CCD) camera (Figure S2). This approach facilitated the visualization and analysis of ECL signals originating from the microbeads while simultaneously discriminating against background noise. Subsequently, to mimic a commercial ECL immunoassay system, the light emission from the functionalized microbeads (Fig. 1) was quantitatively assessed using a photomultiplier tube (PMT) detector [34].

Building upon our prior research [35, 36], this work demonstrates that ECL emission can be obtained when luminol is not free to diffuse, by a synergistic combination of electrode material (BDD) that enables the generation in situ of hydrogen peroxide in carbonate electrolyte, from an applied potential of approximately 2.0 V (vs Ag/AgCl), following the reactions in Scheme 1 [41].

Scheme 1. Reaction mechanism of H_2O_2 formation in carbonate electrolyte (Eqs. 1–3) and ECL emission from luminol (Eqs. 4–7). BDD, electrode reaction site; L, luminol; 3AP, 3-aminophthalate dianion.

$$BDD + OH^- \rightarrow BDD(OH^\bullet) + e^- \quad (1)$$

$$2BDD(OH^\bullet) + 2CO_3^{2-} \rightarrow 2BDD + C_2O_6^{2-} + 2OH^- \quad (2)$$

$$C_2O_6^{2-} + 2H_2O \rightarrow H_2O_2 + 2CO_3^{2-} + 2H^+ \quad (3)$$

$$HO_2^- \rightarrow HO_2^{\bullet} + e^- \quad (4)$$

$$HO_2^{\bullet} \rightleftarrows O_2^{\bullet -} + H^+ \quad (5)$$

$$L + H_2O_2/HO_2^{\bullet}/O_2^{\bullet -} \rightarrow 3AP^* + \text{by products} \quad (6)$$

$$3AP^* \rightarrow 3AP + h\nu \quad (7)$$

Specifically, under basic pH, BDD is capable of oxidizing hydroxide ions to hydroxyl radicals (Eq. 1) [41, 42], which react with carbonate to form peroxydicarbonate ions (Eq. 2), followed by hydrolysis to H_2O_2 (Eq. 3). Subsequently, in basic pH and at potential higher than 1.6 V, hydrogen peroxide is oxidized and partially deprotonated (Eqs. 4–5). All of these reactive oxygen species are capable of reacting with luminol to form an unstable intermediate that spontaneously converts into the excited state of 3-aminophthalate, which returns to the ground state emitting light (Eqs. 6–7) [24, 36]. In conclusion, the ECL emission is triggered primarily by the peculiar electrochemical reaction occurring on the BDD electrode to generate H_2O_2 from carbonate.

As depicted in Fig. 2, ECL images reveal a uniform emission pattern from luminol-functionalized beads, while no emission is observed in the absence of luminol.

In the present experimental setup, luminol is bound onto microbeads, therefore it is not free to diffuse, and the mechanism of luminol emission shall not include its direct oxidation at the electrode, which is the generally accepted mechanism [26, 41, 43].

Figure 3 shows the ECL obtained by cyclic voltammetry when the luminol-labelled microbeads are deposited on a BDD electrode in a carbonate solution.

In agreement with the anticipated effect, restraining the luminol diffusion prevents its oxidation. The typical ECL peak around 0.3–0.5 V (vs Ag/AgCl) was not observed, as we reported previously [41, 44]. However, the ECL started at around 2 V, and we demonstrated that at this potential carbonate oxidation occurs with a consequent production of hydrogen peroxide (Eqs. 1–3) [35, 36], therefore triggering the ECL from luminol (Scheme 1).

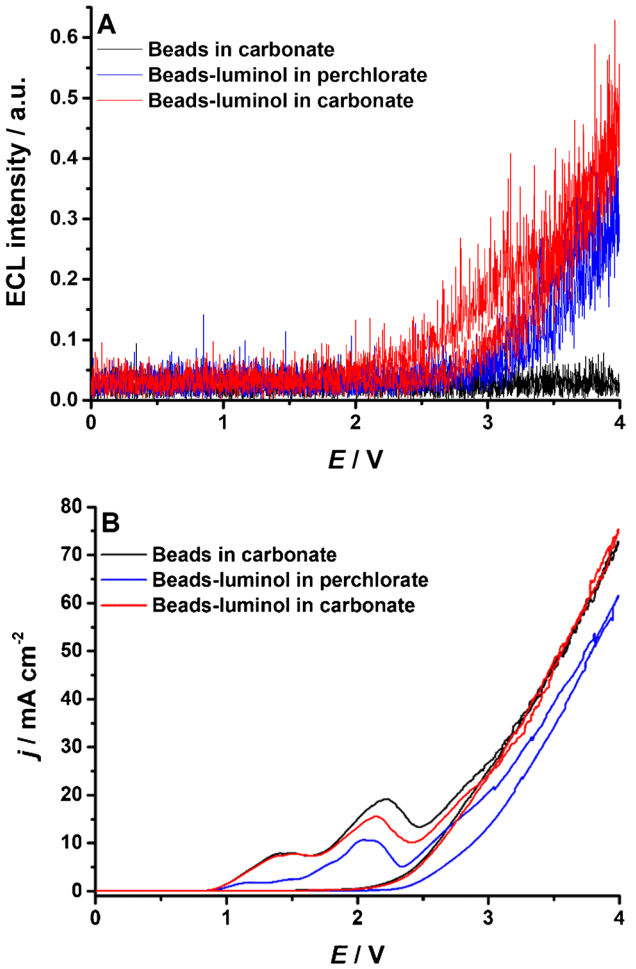

Fig. 3 ECL intensity (**A**) and cyclic voltammetry (**B**). Microbeads in 100 mM Na_2CO_3 (black), microbeads labelled with luminol in 100 mM $NaClO_4$ (blue), and microbeads labelled with luminol in 100 mM Na_2CO_3 (red). The pH is 11.5 for all electrolyte solutions. *E* vs Ag/AgCl (KCl sat.)

Here, we would like to point out that we cannot exclude the oxidation of luminol that can theoretically

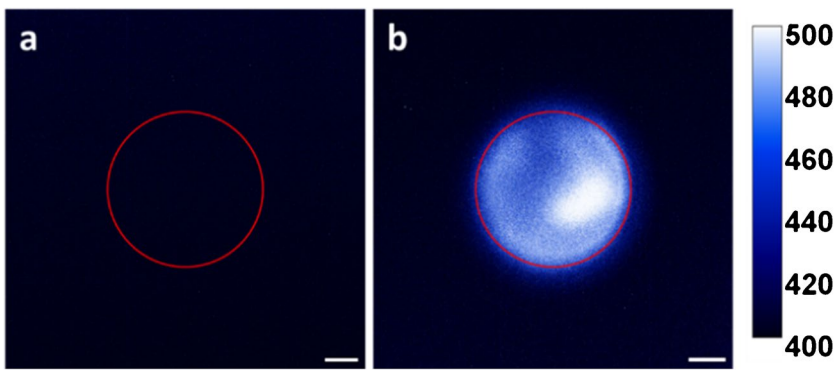

Fig. 2 ECL imaging from luminol-labelled microbeads on BDD electrode as captured with a CCD camera. **a** In 100 mM Na_2CO_3 without luminol microbeads. **b** In 100 mM Na_2CO_3 with 20 µL of luminol-labelled microbeads. The images were obtained by applying a constant potential of 2.5 V (vs Ag/AgCl) for 60 s, integration time of 60 s. The red circle indicates the working electrode active area. Scale bar: 1 mm

occur within the tunneling distance for electron transfer (< 3 nm) [45], but the micrometer diameter of the beads and micrometer roughness of the BDD electrode surface suggest an extremely low probability. In fact, the ECL peak at 0.3–0.5 V (vs Ag/AgCl) was not detected confirming the irrelevance of this electrochemical process in this ECL system. The ineffectiveness of direct electron transfer within the tunneling distance was also proved for microbeads labelled with $Ru(bpy)_3^{2+}$ in the presence of the coreactant peroxydisulfate [46].

Control experiments confirmed that the ECL emission was in fact generated from the luminol. Microbeads without the luminol labelling resulted in background emission only, without any detectable peak confirming the good purity of the ECL system (microbeads and electrolyte), in both carbonate and perchlorate electrolytes. Replacing the carbonate with perchlorate decreased the ECL emission because the amount of hydrogen peroxide produced is lower. The carbonate can be oxidized to peroxydicarbonate, and the following hydrolysis generates hydrogen peroxide, while hydrogen peroxide can be produced only from hydroxide oxidation when perchlorate is the electrolyte, with ECL signals clearly distinguishable from the background (Fig. 4) and reproducible (Figure S3, Table S1).

These results confirm that ECL cannot be obtained at low potentials when luminol is immobilized far from the electrode because it cannot be oxidized electrochemically through direct electron transfer; therefore, any signal observed at lower potentials has to be ascribed to free luminol contamination.

In addition, as luminol is subjected to a chemically irreversible reaction, it has intrinsic low emission compared to metal complexes that are regenerated after the ECL emission.

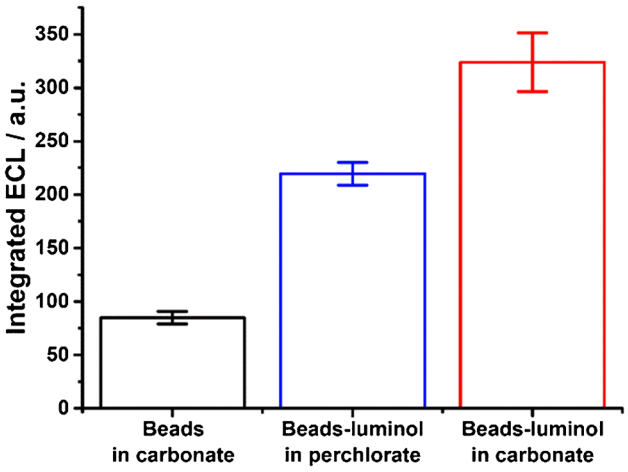

Fig. 4 Integrated ECL intensity: microbeads in 100 mM Na_2CO_3 (black, RSD 6.9%); microbeads labelled with luminol in 100 mM $NaClO_4$ (blue, RSD 4.8%); microbeads labelled with luminol in 100 mM Na_2CO_3 (red, RSD 8.5%). The pH is 11.5 for all electrolyte solutions

Conclusion

Here, we presented a new and until now unknown electrogenerated chemiluminescence emission from luminol when it is labelled on micrometer beads deposited on a boron-doped diamond electrode. By this strategy, luminol is not free to diffuse, and it cannot be oxidized directly at the electrode, preventing the common ECL emission from being observed. We could achieve an ECL emission owing to the special feature of boron-doped diamond electrodes to generate H_2O_2 directly in situ from the oxidation of carbonate.

As a concluding remark, we would like to point out that this ECL system has low emission, inferring little possibility for analytical application at present. Our main aim was to investigate this particular strategy which unveiled a new ECL emission from luminol that has implications in bioanalysis, if the luminol should be immobilized on cells or large biological objects.

Supplementary Information The online version contains supplementary material available at https://doi.org/10.1007/s00216-024-05356-z.

Acknowledgements AF acknowledges the Japan Society for the Promotion of Science (Fellowship ID No. P19333).

Author contribution Conceptualization: Andrea Fiorani. Methodology: Andrea Fiorani, Claudio Ignazio Santo, Kohei Sakanoue. Formal analysis and investigation: Andrea Fiorani, Claudio Ignazio Santo. Writing—original draft preparation: Andrea Fiorani. Writing—review and editing: Andrea Fiorani, Claudio Ignazio Santo, Valenti Giovanni. Funding acquisition: Andrea Fiorani, Yasuaki Einaga. Resources: Andrea Fiorani, Donato Calabria, Mara Mirasoli, Francesco Paolucci, Giovanni Valenti, Yasuaki Einaga. Supervision: Andrea Fiorani.

Funding AF acknowledges the Japan Society for the Promotion of Science for funding this work with Grant-in-Aid for JSPS Fellows, Grant Number 19F19333. GV and FP would like to thank the MIUR, grant numbers 20225P4EJC, P2022E5YSK, and 2020CBEYHC (AStraLI). This work was supported by Nano-ImmunoEra project that has received funding from the European Union's MSCA Staff exchange Horizon Europe programme, grant agreement number 101086341.

Data availability Experimental data are available in AMS acta at https://amsacta.unibo.it/id/eprint/7694.

Declarations

Ethics approval Not applicable.

Source of biological material Not applicable.

Statement on animal welfare Not applicable.

Conflict of interest The authors declare no competing interests.

References

1. Rusling JF, Forster RJ. Biosensors designed for clinical applications. Biomedicines. 2021;9:702.
2. Calidonio JM, Gomez-Marquez J, Hamad-Schifferli K. Nanomaterial and interface advances in immunoassay biosensors. J Phys Chem C. 2022;126:17804–15.
3. Fiorani A, Valenti G, Iurlo M, Marcaccio M, Paolucci F. Electrogenerated chemiluminescence: a molecular electrochemistry point of view. Curr Opin Electrochem. 2018;8:31–8.
4. Yang H, Leland JK, Yost D, Massey RJ. Electrochemiluminescence: a new diagnostic and research tool. Nat Biotechnol. 1994;12:193–4.
5. Richter MM. Electrochemiluminescence (ECL). Chem Rev. 2004;104:3003–36.
6. Miao W. Electrogenerated chemiluminescence and its biorelated applications. Chem Rev. 2008;108:2506–53.
7. Valenti G, Fiorani A, Li H, Sojic N, Paolucci F. Essential role of electrode materials in electrochemiluminescence applications. ChemElectroChem. 2016;3:1990–7.
8. Villani E, Sakanoue K, Einaga Y, Inagi S, Fiorani A. Photophysics and electrochemistry of ruthenium complexes for electrogenerated chemiluminescence. J Electroanal Chem. 2022;921: 116677.
9. Valenti G, Rampazzo E, Kesarkar S, Genovese D, Fiorani A, Zanut A, Palomba F, Marcaccio M, Paolucci F, Prodi L. Electrogenerated chemiluminescence from metal complexes-based nanoparticles for highly sensitive sensors applications. Coord Chem Rev. 2018;367:65–81.
10. Sornambigai M, Bouffier L, Sojic N, Kumar SS. Tris(2,2'-bipyridyl)ruthenium (II) complex as a universal reagent for the fabrication of heterogeneous electrochemiluminescence platforms and its recent analytical applications. Anal Bioanal Chem. 2023;415:5875–98.
11. Haghighatbin MA, Laird SE, Hogan CF. Electrochemiluminescence of cyclometalated iridium (III) complexes. Curr Opin Electrochem. 2018;7:216–23.
12. Suzuki K, Kobayashi A, Kaneko S, Takehira K, Yoshihara T, Ishida H, Shiina Y, Oishi S, Tobita S. Reevaluation of absolute luminescence quantum yields of standard solutions using a spectrometer with an integrating sphere and a back-thinned CCD detector. Phys Chem Chem Phys. 2009;11:9850–60.
13. Barbante GJ, Doeven EH, Kerr E, Connell TU, Donnelly PS, White JM, Lópes T, Laird S, Wilson DJD, Barnard PJ, Hogan CF, Francis PS. Understanding electrogenerated chemiluminescence efficiency in blue-shifted iridium(iii)-complexes: an experimental and theoretical study. Chem Eur J. 2014;20:3322–32.
14. Yeh H-W, Ai H-W. Development and applications of bioluminescent and chemiluminescent reporters and biosensors. Annu Rev Anal Chem. 2019;12:129–50.
15. Fiorani A, Difonzo M, Rizzo F, Valenti G. Versatile electrochemiluminescent organic emitters. Curr Opin Electrochem. 2022;34: 100998.
16. Zhou Y, Villani E, Kurioka T, Zhang Y, Tomita I, Inagi S. Fabrication of luminescent patterns using aggregation-induced emission molecules by an electrolytic micelle disruption approach. Aggregate. 2023;4: e202.
17. Marquette CA, Blum LJ. Applications of the luminol chemiluminescent reaction in analytical chemistry. Anal Bioanal Chem. 2006;385:546–54.
18. Khan P, Idrees D, Moxley MA, Corbett JA, Ahmad F, von Figura G, Sly WS, Waheed A, Hassan MI. Luminol-based chemiluminescent signals: clinical and non-clinical application and future uses. Appl Biochem Biotechnol. 2014;173:333–55.
19. Roda A, Guardigli M. Analytical chemiluminescence and bioluminescence: latest achievements and new horizons. Anal Bioanal Chem. 2012;402:69–76.
20. Villani E, Inagi S. Mapping the distribution of potential gradient in bipolar electrochemical systems through luminol electrochemiluminescence imaging. Anal Chem. 2021;93:8152–60.
21. Villani E, Shida N, Inagi S. Electrogenerated chemiluminescence of luminol on wireless conducting polymer films. Electrochim Acta. 2021;389: 138718.
22. Villani E, Zhang Y, Chen Z, Zhou Y, Konishi M, Tomita I, Inagi S. AC-bipolar electrosynthesis and luminol electrochemiluminescence imaging of poly(3,4-ethylenedioxythiophene) and its composite films. ACS Appl Polym Mater. 2023;5:6186–98.
23. Hiramoto K, Komatsu K, Shikuwa R, Konno A, Sato Y, Hirano-Iwata A, Ino K, Shiku H. Evaluation of respiratory and secretory activities of multicellular spheroids via electrochemiluminescence imaging. Electrochim Acta. 2023;458: 142507.
24. Zhou P, Hu S, Guo W, Su B. Deciphering electrochemiluminescence generation from luminol and hydrogen peroxide by imaging light emitting layer. Fundam Res. 2022;2:682–7.
25. Feng M, Dauphin AL, Bouffier L, Zhang F, Wang Z, Sojic N. Enhanced cathodic electrochemiluminescence of luminol on iron electrodes. Anal Chem. 2021;93:16425–31.
26. Sakura S. Electrochemiluminescence of hydrogen peroxide-luminol at a carbon electrode. Anal Chim Acta. 1992;262:49–57.
27. Rahmawati I, Einaga Y, Ivandini TA, Fiorani A. Enzymatic biosensors with electrochemiluminescence transduction. ChemElectroChem. 2022;9: e202200175.
28. Miao W, Choi J-P, Bard AJ. Electrogenerated chemiluminescence 69: the Tris(2,2'-bipyridine)ruthenium(II), $(Ru(bpy)_3^{2+})$/Tri-*n*-propylamine (TPrA) system revisited - a new route involving $TPrA^{\bullet+}$ cation radicals. J Am Chem Soc. 2002;124:14478–85.
29. Sentic M, Milutinovic M, Kanoufi F, Manojlovic D, Arbault S, Sojic N. Mapping electrogenerated chemiluminescence reactivity in space: mechanistic insight into model systems used in immunoassays. Chem Sci. 2014;5:2568–72.
30. Zanut A, Fiorani A, Canola S, Saito T, Ziebart N, Rapino S, Rebeccani S, Barbon A, Irie T, Josel H-P, Negri F, Marcaccio M, Windfuhr M, Imai K, Valenti G, Paolucci F. Insights into the mechanism of coreactant electrochemiluminescence facilitating enhanced bioanalytical performance. Nat Commun. 2020;11:2668.
31. Chen L, Hayne DJ, Doeven EH, Agugiaro J, Wilson DJD, Henderson LC, Connell TU, Nai YH, Alexander R, Carrara S, Hogan CF, Donnelly PS, Francis PS. A conceptual framework for the development of iridium(III) complex-based electrogenerated chemiluminescence labels. Chem Sci. 2019;10:8654–67.
32. Zanut A, Fiorani A, Rebeccani S, Kesarkar S, Valenti G. Electrochemiluminescence as emerging microscopy techniques. Anal Bioanal Chem. 2019;411:4375–82.
33. Sojic N. Analytical electrogenerated chemiluminescence: from fundamentals to bioassays; Royal Society of Chemistry (RSC) Publishing, 2019.
34. Sakanoue K, Fiorani A, Santo CI, Irkham, Valenti G, Paolucci F, Einaga Y. Boron-doped diamond electrode outperforms the state-of-the-art electrochemiluminescence from microbeads immunoassay. ACS Sens. 2022;7:1145–1155.
35. Irkham, Fiorani A, Valenti V, Kamoshida N, Paolucci F, Einaga Y. Electrogenerated chemiluminescence by in situ production of coreactant hydrogen peroxide in carbonate aqueous solution at a boron-doped diamond electrode. J Am Chem Soc. 2020;142:1518–1525.
36. Irkham, Rais RR, Ivandini TA, Fiorani A, Einaga Y. Electrogenerated chemiluminescence of luminol mediated by carbonate electrochemical oxidation at a boron-doped diamond. Anal Chem. 2021;93:2336–2341.
37. Rebeccani S, Zanut A, Santo CI, Valenti G, Paolucci F. A guide inside electrochemiluminescent microscopy mechanisms for analytical performance improvement. Anal Chem. 2021;94:336–48.

38. Knezevic S, Bouffier L, Liu B, Jiang D, Sojic N. Electrochemiluminescence microscopy: from single objects to living cells. Curr Opin Electrochem. 2022;35: 101096.
39. Sakanoue K, Fiorani A, Irkham, Einaga Y. Effect of boron-doping level and surface termination in diamond on electrogenerated chemiluminescence. ACS Appl Electron Mater. 2021;3:4180–4188.
40. Pollok NE, Rabin C, Smith L, Crooks RM. Orientation-controlled bioconjugation of antibodies to silver nanoparticles. Bioconjugate Chem. 2019;30:3078–86.
41. Marselli B, Garcia-Gomez J, Michaud P-A, Rodrigo MA, Comninellis Ch. Electrogeneration of hydroxyl radicals on boron-doped diamond electrodes. J Electrochem Soc. 2003;150:D79–83.
42. Henke AH, Saunders TP, Pedersen JA, Hamers RJ. Enhancing electrochemical efficiency of hydroxyl radical formation on diamond electrodes by functionalization with hydrophobic monolayers. Langmuir. 2019;35:2153–63.
43. Haapakka KE, Kankare JJ. The mechanism of the electrogenerated chemiluminescence of luminol in aqueous alkaline solution. Anal Chim Acta. 1982;138:263–75.
44. Rahmawati I, Saepudin E, Fiorani A, Einaga Y, Ivandini TA. Electrogenerated chemiluminescence of luminol at a boron-doped diamond electrode for the detection of hypochlorite. Analyst. 2022;147:2696–702.
45. Imai K, Valenti G, Villani E, Rapino S, Rampazzo E, Marcaccio M, Prodi L, Paolucci F. Numerical simulation of doped silica nanoparticle electrochemiluminescence. J Phys Chem C. 2015;119:26111–8.
46. Zhou P, Fu W, Ding L, Yan Y, Guo W, Su B. Toward mechanistic understanding of electrochemiluminescence generation by tris(2,2'-bipyridyl)ruthenium(II) and peroxydisulfate. Electrochim Acta. 2023;439:141716.